Forecasting the Depth of Failure in Underground Development

G. Sweby[1(✉)], P. Brenchley[2], P. Novomodny[1], J. Player[1], and A. Sacco[1]

[1] MineGeotech P/L, Perth, WA, Australia
gordonsweby@minegeotech.com.au
[2] 29Metals, Perth, WA, Australia

Abstract. A back-analysis case study is presented whereby the depth-of-failure in the rockmass surrounding underground development was correlated with borehole camera measurements. The case study took place at the Golden Grove Underground Mine (29 Metals) at a depth of ~1150–1400 m with moderately complex geology. Purpose designed holes were drilled into the backs and walls at ~420 locations in various lithologies including intrusive dykes, then video recordings using a forward-looking borehole camera were made for office study and analysis. The depth-of-failure, where observable, was recorded and compared against inelastic numerical model (RS3) outputs to determine the appropriate parameters for forward analysis. A regression analysis approach was then used to determine the value of the parameter which best fit the data. It was found that the Maximum Shear Strain parameter was the best fit to observations in the foliated host rockmass, while the Extension Strain parameter fit observations in the intrusive dykes best. The study has positioned the operation well for making forecasts of future rockmass damage at increasing depth, thereby improving confidence in their mining reserve.

Keywords: Model forecasting · Damage mapping · Inelastic modelling

1 Introduction

The depth-of-failure surrounding an underground excavation is an important parameter in the design of both static and dynamic ground support, as it dictates the demand (load) of the system. It also dictates the length of the reinforcing tendon required for static (deadweight) calculations. The designer is faced with many available options for determining the depth of failure based on kinematics, empirical and numerical modelling approaches.

In this paper, a case study is presented where observational methods are used to refine criteria for forecasting depth-of-failure using three-dimensional finite-element modelling. Borehole camera images were used to determine a 'depth-of-damage' based on observed fracture limits. These limits were compared to model outputs to provide the best-fit match based on a least-squares minimisation process. The best-fit parameters determined in this process can be used for making forward predictions about the damage envelopes that can be expected in other parts of the mine and at greater depth.

R. E. Hammah et al. (Eds.): RIC 2023, AHE 19, pp. 478–490, 2023.
https://doi.org/10.2991/978-94-6463-258-3_47

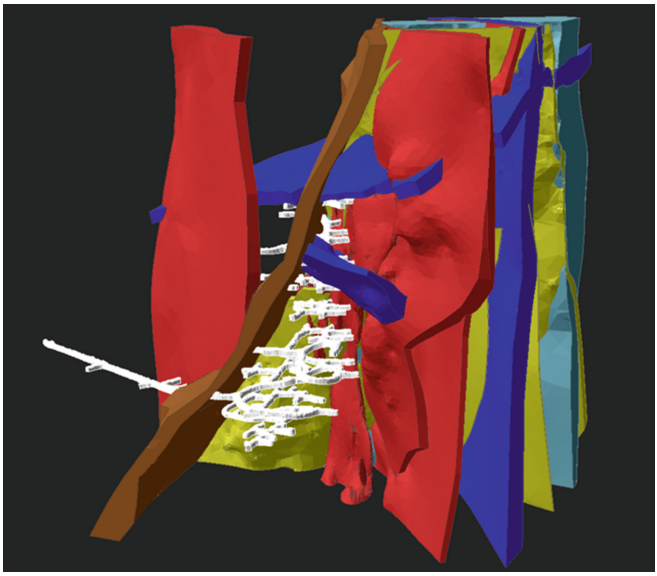

Fig. 1. Geological model of the case-study area of mine development (white). Red = Dacite, Blue = Dolerite, Yellow = Rhyolite, Brown = Fault).

The case study took place at Golden Grove Operation, a metalliferous mine located in the Yilgarn Craton of Western Australia, at a depth of ~1300 m below surface.

2 Local Geology

The host rockmass can be described as a tuffaceous debris of rhyolite to andesite composition, inter-bedded with minor sedimentary bands and volcanics ranging from andesite to rhyodacite. The individual lithology units within the overall stratigraphic horizon have variable strength but cannot be individually considered due to a lack of continuity across the deposit. This gives rise to a wide distribution of intact rock strength (Sect. 3).

Dyke-like dacite, dolerite and rhyolite bodies, with varying thickness and orientation, cut through the host formations in the study area (Fig. 1).

A significant (10–20 m wide) regional fault zone (the Catalpa Fault) bounds the study area (brown in Fig. 1) and is the source of significant historic seismic activity.

3 Geotechnical Characteristics

The host rockmass consists of interbedded massive and foliated zones, with the foliated zones exhibiting strong anisotropy giving rise to slabbing in the walls of N-S oriented development (Fig. 2 and Fig. 3). The intact rock strength is highly variable, averaging 133 MPa with a standard deviation of 61 MPa. The Mohr-Coulomb strength of the anisotropy, as determined by analysis of triaxial samples which failed along foliation, is 28 MPa (cohesion) and 25° (friction).

Fig. 2. Anisotropic host rockmass, steep foliation subparallel to N-S oriented walls.

Fig. 3. Buckling in sidewalls due to combination of stress and foliation.

The intrusives vary in strength, depending on their composition, but are all significantly stronger than the host rockmass, as given in Table 1.

The relative intact moduli of the intrusives also indicates that these units are markedly stiffer than the host rockmass (Table 2).

The key geotechnical characteristics thus captured in the numerical model, are summarised in Table 3. All materials except for the host were modelled as isotropic and a Geological Strength Index (GSI) of 80 was used for all domains.

Table 1. Intact Strength of Modelled Domains

Geotechnical Domain	Number of Tests	Mean UCS (MPa)	Standard Deviation UCS (MPa)
Host Rockmass	138	133	61
Dacite	37	214	47
Dolerite	22	179	56
Rhyolite	28	240	80

Table 2. Modulus determined by transducer on triaxial test samples

Geotechnical Domain	Modulus (GPa)
Host rockmass	35.5
Dacite Intrusive	44.0
Dolerite Intrusive	45.0
Rhyolite Intrusive	40.0

Table 3. Geotechnical strength characteristics for model input

Geotechnical Domain	Hoek-Brown UCS (MPa)	Hoek-Brown mi	Mohr-Coulomb Cohesion (MPa)	Mohr-Coulomb Friction (°)	Modulus (GPa)
Host	133	13.5	28	25	35.5
Dacite	214	19	n/a	n/a	44
Dolerite	179	22	n/a	n/a	45
Rhyolite	240	15	n/a	n/a	40
Fault Zone	308	8.5	28	25	43

4 In Situ Stress

Hollow-Inclusion (HI) Cell measurements exist at the site, with orientations as given in Fig. 4. The stress tensor based on these measurements are given in Table 4.

A LIDAR scan carried out on a vertical raise bored shaft near the study area exhibited spalling (dog-earing) which is an accurate indicator of the maximum stress orientation in the plane perpendicular to the shaft axis. A camera image of the spalling (Fig. 5) and a cross-section through a dog-eared zone (Fig. 6) clearly indicate a maximum stress orientation of ~60° (~90° to the measured maximum principal stress). A review of available raisebore breakout measurements from other parts of the mine (Fig. 7) also indicated a S1 orientation roughly perpendicular to the measured (HI) stress field.

Final confirmation of the major principal stress orientation was achieved by considering the orientation of core discing saddles where the discs had a pronounced curvature.

Table 4. Measured In Situ Stress Field

Principal Stress	k-ratio	Orientation	Value at Model Centroid (MPa)
Maximum (S1)	2.7	150	99.1
Intermediate (S2)	2.1	060	77.1
Minimum (S3)	-	Vertical	36.7

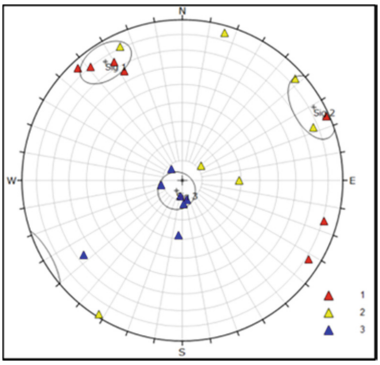

Fig. 4. Measured Stress Field (HI Cell).

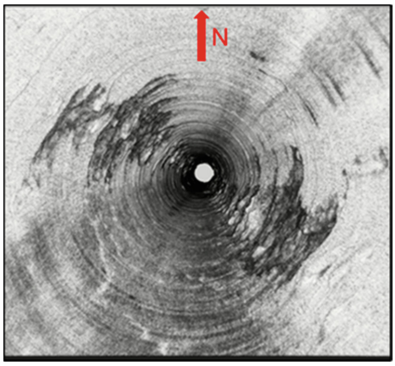

Fig. 5. Spalling – vertical raisebored shaft.

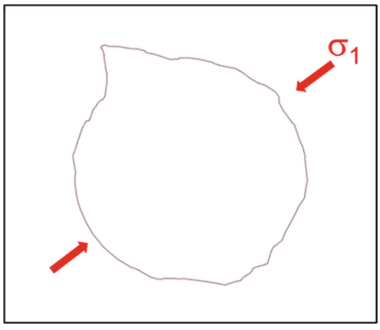

Fig. 6. Cross-section: Lidar Scan.

It has been found [1] that the alignment of the discing saddle base corresponds to the orientation of the maximum stress in the plane perpendicular to the core axis, as illustrated in Fig. 8.

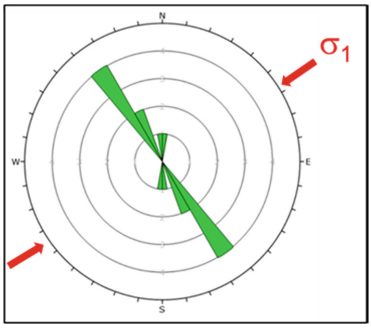

Fig. 7. Historic raisebore breakout.

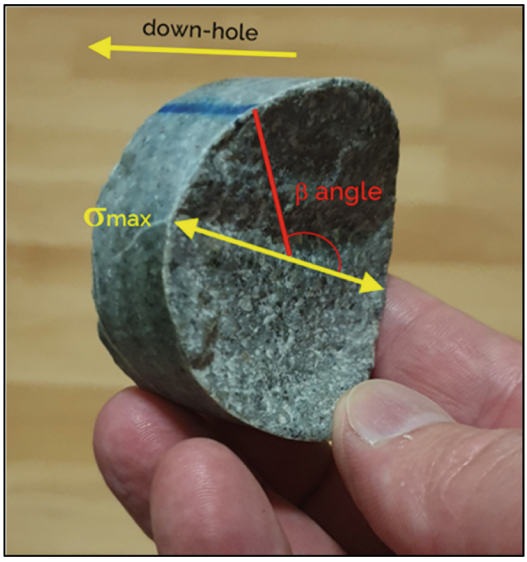

Fig. 8. Discing saddle measurement.

By simulating the expected discing saddle orientation based on the measured (HI) stress field versus the observed orientation, using a 3D model of the borehole at its surveyed orientation, it was possible to eliminate the measured stress field as the least likely of the two possible orientations Fig. 9.

Taking into consideration all the above observational data, the stress field used in the analysis was modified as given in Table 5.

5 Borehole Camera Observations

A total of 420, 3 m long, jumbo-drilled percussion holes were drilled into the backs and walls at various locations throughout the study area (Fig. 10). The holes were then probed with a forward-looking borehole camera and a video recorded for office analysis.

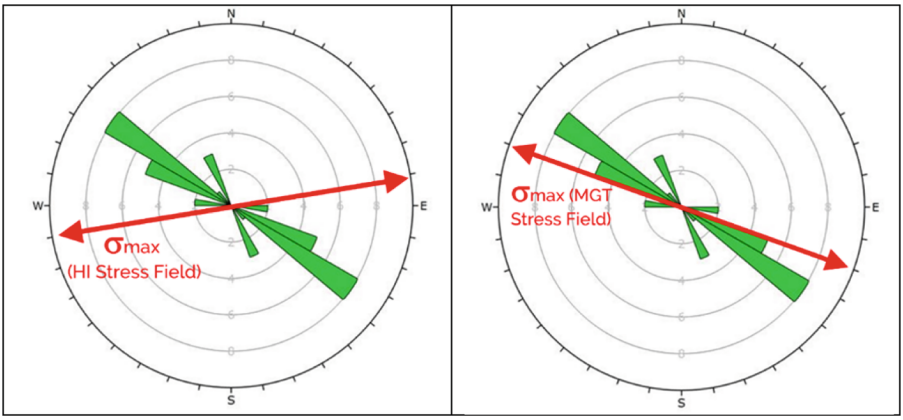

Fig. 9. Discing saddle measurements (green) versus predictions based on stress field (red).

Table 5. Modified In Situ Stress Field

Principal Stress	k-ratio	Orientation	Value at Model Centroid (MPa)
Maximum	2.7	060	99.1
Intermediate	2.1	150	77.1
Minimum	-	Vertical	36.7

The intent is to re-survey all the accessible holes once stoping is complete, to record the difference in damage depth, however this part of the study is still underway.

Example images from the borehole camera, illustrating the style of fracturing observable using this technique, are given in Fig. 11. The general rockmass conditions and ground support scheme installed at each site were also recorded for inclusion in the analysis.

6 RS3 Model

A 3D inelastic finite-element model was built in RS3 [2], to capture the key geotechnical components affecting the development of damage around the development excavations. The lithological units are as shown in Fig. 1 and the development/stoping as shown in Fig. 12. The physical dimensions of the model are ~1.8 km × 1.8 km in plan, and ~2 km in vertical extent. Approximately 20 million mesh elements were used to provide the required resolution around the excavations.

The strength parameters used for the respective lithological units are as given in Table 6. To capture the anisotropic behaviour of the foliated host rock mass and the fault zone, anisotropic surfaces were used to define the direction of preferential shear and are shown in Fig. 13. The fault zone shear strength input parameters are as given in Table 6.

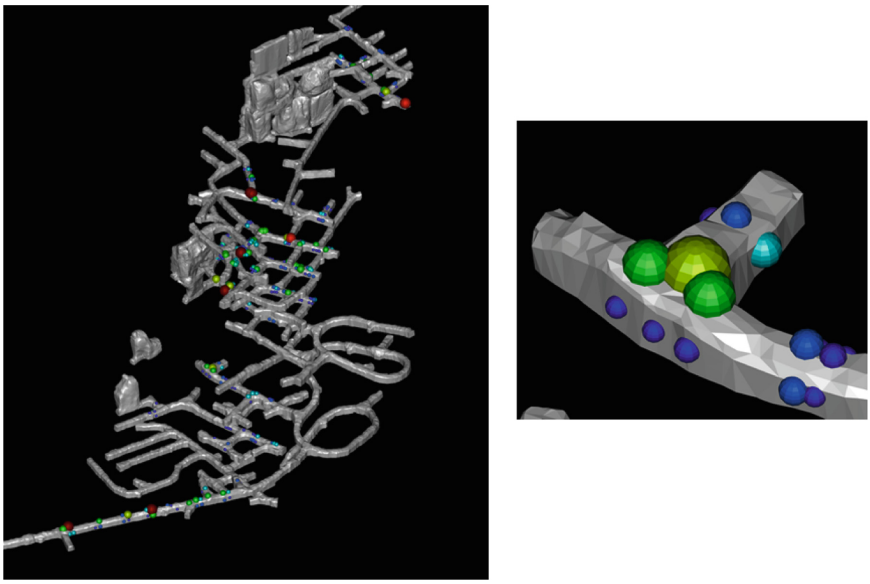

Fig. 10. Borehole Camera Observation Hole Locations (spheres coloured and sized according to damage depth).

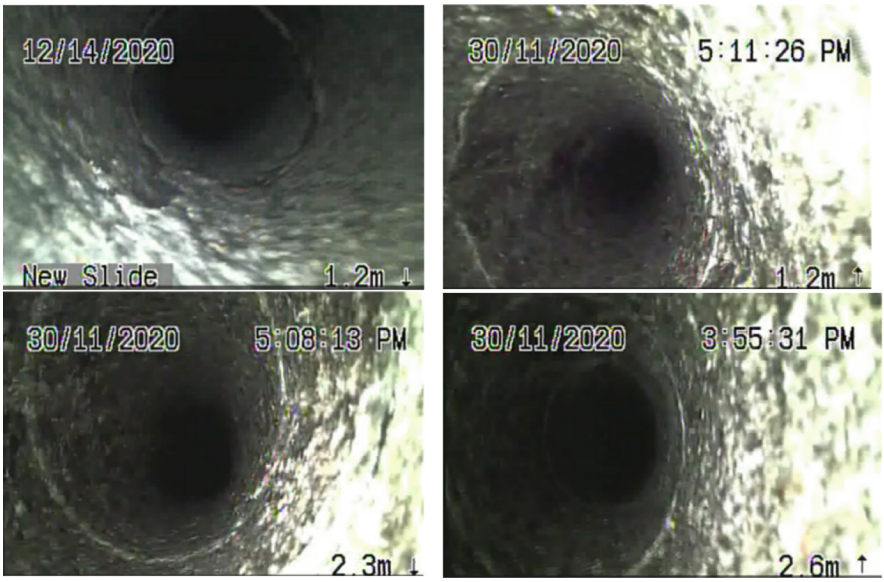

Fig. 11. Borehole Camera Images – Fractures perpendicular to borehole axis.

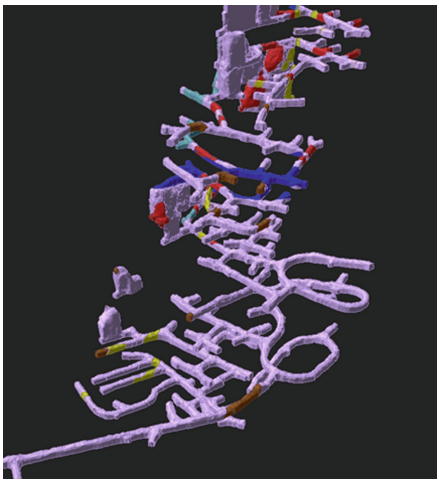

Fig. 12. Development and stoping voids captured in the RS3 model, coloured by domain.

Table 6. Model Strength Input Parameters

Geotechnical Domain	Hoek-Brown UCS (MPa)	PeakRock Mass Hoek-Brown mb	Residual Rock Mass Hoek-Brown mr	Mohr-Coulomb Cohesion (MPa)	Mohr-Coulomb Friction (°)	Rock Mass Modulus (GPa)
Host	133	6.6	1	28	25	31
Dacite	214	9.3	1.5	n/a	n/a	39
Dolerite	179	10.8	1.7	n/a	n/a	40
Rhyolite	240	7.3	1.1	n/a	n/a	35
Fault Zone	308	4.9	0.7	28	25	38

7 Methodology

To account for the errors inherent in this process, due to factors such as:

- Fracture depth measurement (forward-looking borehole camera)
- Mesh size (varies from location to location in model)
- Material property inherent variability
- Simplified excavation geometry (from underground manual survey rather than scan)

a statistical approach has been adopted, whereby the 'best fit' of a model output parameter to the observed dataset has been determined.

A trial-and-error approach was initially carried out to determine the output parameter that best fit the data, based purely on visual inspection. Based on this initial review, the parameters selected for further analysis were:

1. Extension Strain – applicable to backs and walls of development in intrusives

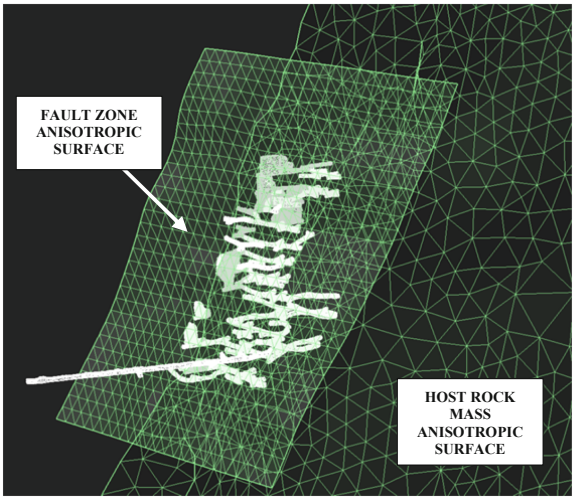

Fig. 13. Anisotropic surfaces defining the foliation orientation in the host rockmass and the fault zone.

2. Maximum Shear Strain – applicable to backs and walls of development in foliated host

Isosurfaces corresponding to a range of values for each parameter were generated for comparison with the measured observations.

By minimizing the sum of squares of the difference between observed and predicted at each borehole location in the model, it was possible to determine the 'least-squares' best-fit to the data.

8 Results

Using GEM4d software [3] the observations were represented by spheres approximately scaled to the depth of fracturing (Fig. 14). The model forecast strain isosurface is then overlain for a preliminary determination of the 'ballpark' best-fit range (Fig. 15).

It was found that two criteria are required, for the backs and the walls respectively Fig. 16. Also, the maximum shear strain criterion was not found to fit the observations for the intrusive domains, rather the extension strain criterion [4] proved a more reliable fit.

Plots summarizing the results of the minimization analysis to determine the 'optimal' strain criteria are given in Fig. 17. The resulting 'best-fit' parameters are given in Table 7 and can be used for forecasting conditions in other parts of the mine and for future ground control planning.

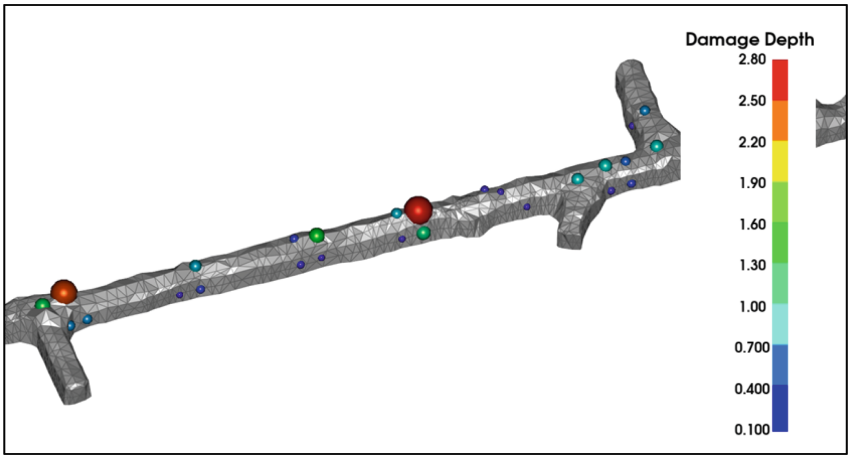

Fig. 14. Development segment showing location of monitoring boreholes with the size of the sphere scaled relative to the depth of fracture recorded.

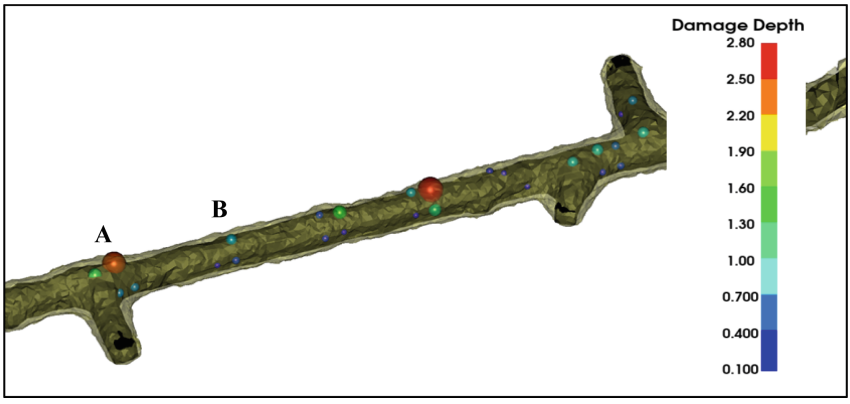

Fig. 15. Maximum Shear Strain isosurface superimposed on the development, providing a means to 'eyeball' the range in values best matching the observations.

9 Conclusions

A methodology for determining model output parameters for forecasting depth of damage around development excavations at a deep level base metals mine has been presented.

The values of Maximum Shear Strain and Extension Strain presented in Table 7 are now used at this site to make forecasts about damage depth in other parts of the mine and at greater depths. This is a very useful aid to planning future ground control requirements.

The correlation between measured and modelled dimensions is not good, thus a methodology for determining the best-fit using the least-squares approach was required.

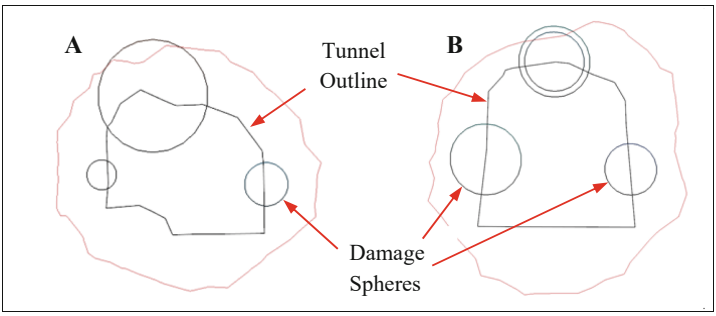

Fig. 16. Sections through the development at positions A and B (in Fig. 15 indicating a reasonable fit to the observations in the backs, but a poor fit in the walls.

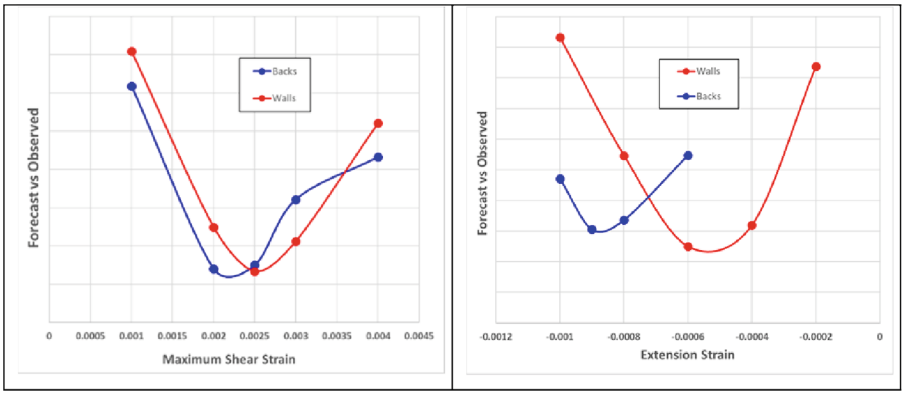

Fig. 17. Minimisation of the sum of the squares of the difference between observed and forecast.

Table 7. Best-fit strain parameters

Geotechnical Domain	Maximum Shear Strain	Extension Strain
Foliated Host - Backs	0.0022	-
Foliated Host - Walls	0.0025	-
Intrusives - Backs	-	−0.0009
Intrusives - Walls	-	−0.00055

The criteria in Table 7 can be considered optimal, but large variances can be expected due to the uncertainties inherent in the rockmass, the excavation shape and the measurement technique itself.

Future study will focus on correlating the magnitude of strain forecast at the excavation surface with a locally developed rockmass damage classification scheme.

References

1. Basson, F.: GEM4D computer software (2023).
2. Dyke, C.G.: Core discing: its potential as an indicator of principal in situ stress directions. In: ISRM International Symposium. OnePetro (1989)
3. Rocscience Incorporated: RS3v4.026 3D finite element analysis program for modelling slopes, tunnel and support design, surface and underground excavations. Rocscience, Ont, Canada
4. Stacey, T.R.: A simple extension strain criterion for fracture of brittle rock. International Journal of Rock Mechanics and Mining Sciences & Geomechanics Abstracts. Vol. 18. No. 6 Peragmon